An Experimental Study of On-line Estimation of Striations in Laser Cutting Process

Paul Di Pietro
Di Pietro and Sons Engineering
Fairy Meadow, NSW, Australia

Kai Chen, Y. Lawrence Yao
Department of Mechanical Engineering
New York, NY, USA

ABSTRACT

Striation formation on laser made cuts results in poorer surface finish and post-cut operation often becomes necessary as a result. Proper process planning reduces, but not eliminate striations, and on-set or characteristic changes of striations in process has routinely been observed. On the basis of high speed filming and pyrometer investigations, experiments were carried out using a photodiode based sensing system. Signals are analyzed using both parametric and spectral methods and results show agreement with measured striation data. The experimental results also agree with previous theoretical calculations.

INTRODUCTION

There have been many research efforts undertaken previously in order to understand and hence improve laser cutting quality, as reviewed by Di Pietro and Yao in 1994. In particular, the formation of striations have received much attention because it has been shown to strongly affect the quality of laser cutting. Striations appear on the cut edge as relatively regular straight lines, when reasonable laser parameters are selected. A more complex pattern is observable when such parameters are incorrectly determined and poor quality cutting often occurs as a result (Fig. 1).

Many explanations have been given to stria occurrence. It has been shown theoretically that the liquid layer can oscillate with a natural frequency, prior to its ejection out of the bottom of the kerf (Schuocker, 1986, 1987). The results obtained for the natural frequency have correlated reasonably with experimental work. It does not explain why striations are much more pronounced in reactive gas assisted laser cutting than in inert gas cutting.

Another explanation suggests that at cutting speeds less than the critical reaction rate, sideways burning occurs and results in the periodic forming of striations (Arata, 1979). High speed photography was used to visualize this mechanism at speeds below the reaction speed. Recently, more work has been carried out (Ivarson, *et al.*, 1994) and it is suggested that the critical reaction rate is limited by the diffusion rate of oxygen into the melt, brought about by changes in the oxygen partial pressure gradient in the cut zone.

In Di Pietro and Yao (1995), it is argued that neither the sideways burning theory nor the liquid layer oscillation theory can be dispelled. At speeds less than the reaction front, both mechanisms occur simultaneously with sideways burning being predominant, whilst at higher speeds above the reaction front speed, sideways burning ceases and liquid layer oscillations become relatively pronounced. More recently (Chen and Yao, 1996), it was shown that, as thickness of the molten layer increases with speed, the stability of the layer improves.

[1] Author to whom all correspondence should be addressed

Striation formation is a complex phenomenon. Striation patterns in terms of frequency and depth may change gradually or suddenly in process even under constant conditions. The exact cause(s) for such change are not fully understood. In some cases, such change has been associated with changing boundary conditions, such as boundary encroachment where heat dissipation reduces. In other cases, such change may be caused by necessary process parameter changes, such as speed change required for cornering or contouring. In cases where there appear no apparent reasons for such change, it is often attributed to laser source fluctuation, plasma change, or non-uniformity in material properties.

It is therefore the objective of this study to investigate effective sensing and signal processing techniques for on-line detection and estimation of striations based on the improved understanding of the mechanisms. This is useful in un-manned operation of industrial cutting systems, whereby operators can be alerted when cutting quality falls below control limit acceptability.

PREPARATORY WORK

The laser source used is of CO_2 type with a maximum power of 1.5 kW. The beam mode used is TEM_{00}. Continuous wave (CW) operation was used for all experiments. The beam was focused down to 250 µm through a 5" ZnSe lens. The throat diameter of the adjustable nozzle was 1 mm and a standoff distance of 1 mm was also maintained. Assist gas pressures were kept constant at 2.7 bar unless otherwise noted. Cold rolled mild steel sheet of 1 mm thickness were used. The accuracy of the commanded laser power was examined by a power probe. Fig. 2 shows the power levels measured by the probe and its associated discharge current for one of eight discharges. Current control is via a 12 bit digital word which allows accurate manipulation through part programs generated or through the manual data input. An accuracy of 5% of reading and a repeatability of 1.5 % was found.

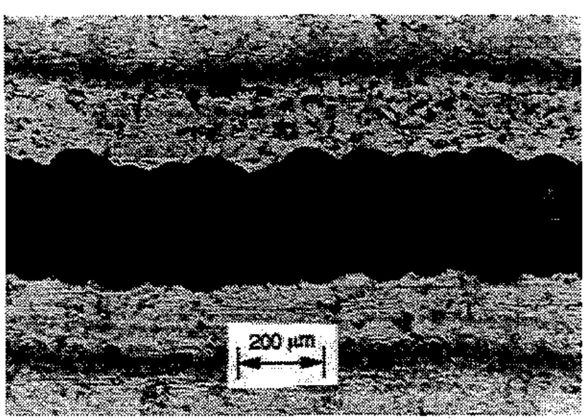

Fig. 1 TYPICAL STRIATION FORMATION (CO_2 500W, 30 mm/s, OXYGEN 2.1 BAR)

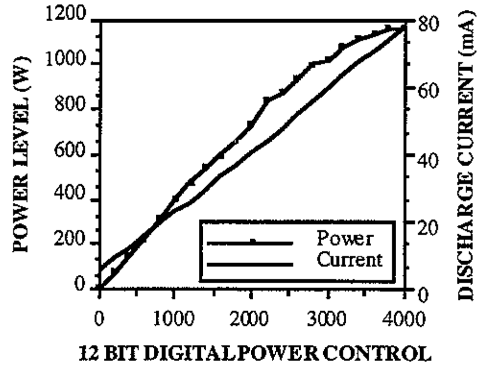

Fig. 2 POWER LEVELS VS. DISCHARGE CURRENT & DIGITAL CONTROL WORLD

It has been suggested that motion or handling systems can influence the surface morphologies of cuts produced (Biermann, 1988). In order to assess the performance of the handling system installed, vibration thereof was measured using an accelerometer. Cuts were produced at various speeds whilst maintaining constant power levels. It was ascertained that the vibration characteristics of the handling system did not correlate to any of the actual striation frequencies measured. Fig. 3 shows a power spectrum of the table vibration produced when straight cutting a 1 mm thick mild steel sample at 33 mm/sec with 600 W of beam power. Two significant fundamental frequencies were identified at 70 Hz and 94 Hz, which translate into significant harmonics. Some of these harmonics tended to superimpose each other at frequencies of approximately 281 Hz, 562 Hz, and 842 Hz. Of these, by far the most significant vibration level was identified at 842 Hz, which is higher for the production of striations in general. The actual striation frequency measured was 320 Hz, and it can clearly be seen that in the band which encompasses this frequency (between approximately 180 Hz and 350 Hz), suppressed vibration levels are found.

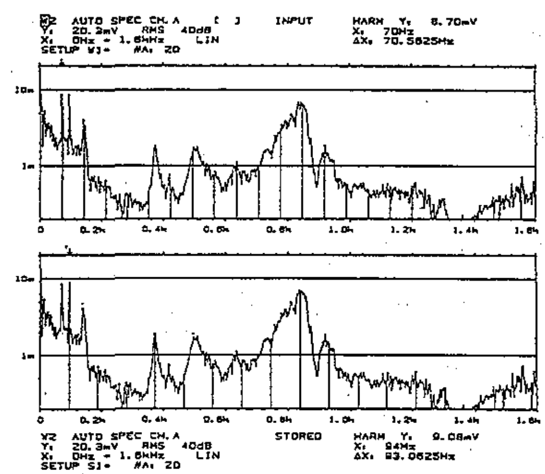

Fig. 3 TYPICAL VIBRATORY CHARACTERISTICS OF THE MOTION SYSTEM (SPEED 33 mm/s)

ASSESSING SENSING SYSTEM

In order to assess a suitable sensing system for obtaining signals from which striation frequency and roughness depth can be obtained, high speed photography was undertaken to view the interaction zone. The camera (Hitachi 16HM - HIMAC) was focused directly on the laser-material interaction zone. It was positioned perpendicular to the line of cut at an angle of 15° from horizontal, so that any lateral movement of the front (in the direction of the cut) can easily be discerned. Kodak - Ektachrome 7240, 16 mm by 100 ft (30.5 m) double perforated color positive film was used. A timing light pulse generator operated at a rate of 100 pulses/s (width 170 µS) was used to overcome the problem of camera acceleration to reach pre-set levels. Actual film speeds can then be easily calculated. To minimize flickering in AC operated lights, two special photographic lamps of 500 W each were used to illuminate the workpiece.

Fig. 4 shows a portion of the film (500 frames/s) developed under steady-state process conditions when cutting was carried out using 600 W of beam power at a speed of 20 mm/s. The apparent periodicity was previously explained using the sideways burning theory proposed by Arata in 1979 and each cycle consists extinction, ignition, and burning. In this case, the cycle time of this phenomenon is 6 ms, or occurs at a frequency of 166.7 Hz. The actual workpiece edge was examined using a microscope and a striation frequency of 162.8 Hz was found. The good agreement indicates frequency of the light intensity change can be reasonably correlated with the actual striation frequency.

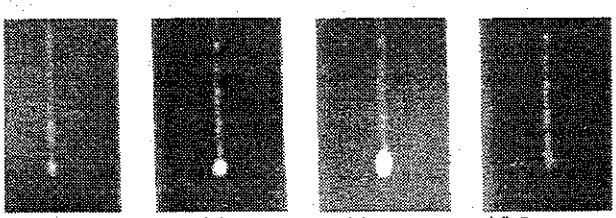

(a) 0 ms (b) 2 ms (c) 4 ms (d) 6 ms

Fig. 4 HIGH SPEED PHOTOGRAPHS TAKEN WITH A FRAME INTERVAL OF 2ms (CUTTING SPEED: 20 mm/s, LASER POWER: 600 W)

Analysis of the developed film was carried out under a Nikon Shadowgraph facilitated with digital micrometers. Fig. 5 quantifies the magnitude of the cutting front mobility (i.e., the maximal fluctuation in diameter of a bright spot) to be about 200 µm. This correlates reasonably with the maximum roughness height obtained under similar cutting conditions (Di Pietro and Yao, 1995). This quantification shows the extent of spot size fluctuation can be correlated reasonably with the roughness height, even though there is some experimental variation due to factors like camera resolution.

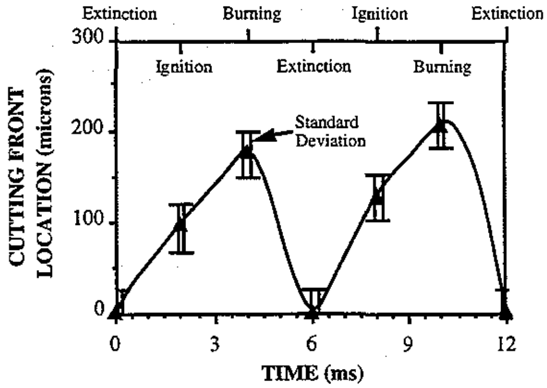

FIG. 5 TYPICAL CUTTING FRONT MOBILITY MEASURED BY HIGH SPEED PHOTOGRAPHY (CUTTING SPEED: 20 mm/s, LASER POWER: 600 W, FRAME RATE: 500 FRAMES/s))

The high speed photography work was dependent on light emission from the interaction zone. In addition, it was sensitive enough to observe the ignition-burning-extinction, matched the actual striation frequency produced on the cut edge, and related to the measured roughness heights. It follows then that some sort of radiation detector which is highly sensitive to light emission fluctuations, would be appropriate to detect striation frequency and roughness depth on-line.

Laser cutting results in a visible yellow/orange colored emission although CO_2 laser itself is invisible. Stefan-Boltzman's equation expresses integrated or total energy emitted by an irradiating surface:

$$\ddot{q}_{rad} = \varepsilon \sigma_b T^4 \ (W/m^2). \qquad (1)$$

where ε is dimensionless emissivity, σ_b the Stefan-Boltzman's constant. For a constant temperature, Wien's displacement law finds the point of maximum emissive power:

$$\Omega_{max} T = 2897.8 \ \mu m.K. \qquad (2)$$

The wavelength Ω_{max} identified represents the dominant radiation component in the emission. In order to assess the range of wavelengths to be detected by the sensor, typical temperature ranges experienced in laser cutting required investigation. An infrared non-contact temperature measurement system was utilized for this purpose (Raytek - Thermalert 30 controller). Because the spot size is 0.95 mm (at a standoff distance of 127 mm) which is much larger than the cutting front, the pyrometer was calibrated by the following method. Two mild steel samples were heated by the unfocused laser beam at a power level of 160 W for 2 min. One of the samples contained a laser cut with a kerf width of 250 µm whilst the other did not contain a cut. This was repeated several times and a reading calibration ratio of 1.3 was achieved. Fig. 6 shows the temperatures obtained from the calibrated sensing system. The sensor selected to achieve this was a BPX 65 high speed photodiode. This is a 1 mm^2 planar silicon PIN photodiode housed in a hermetically sealed TO - 18 case, incorporating an integral plain glass window.

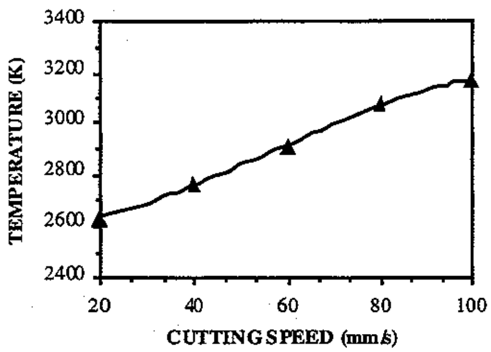

FIG. 6 CUTTING FRONT TEMPERATURES BY PYROMETRY (EMISSIVITY: 0.4, LASER POWER: 600 W)

EXPERIMENTAL SETUP

The photodiode has a maximum peak sensitivity at 850 nm (bandwidth: 400 to 1064 nm). A risetime of typically 0.5 ns (1 ns max.) is achievable, with a cut-off frequency of 500 Mhz. When reverse biased, the leakage current increases proportionally with the incident light. A cylindrical black-coated light shield was fitted to the diode and was bracket mounted 200 mm away from the cutting front. Again a declivity of 15° was made relative to the workpiece, whilst viewing light emissions along the line of cut. To minimize signal corruption by the ejected spark-shower (reflecting off the bottom of the cutting box), templates were made up to completely surround the workpiece. In addition, the signal is also uncontaminated by any reflected CO_2 laser radiation as its wavelength (10.6 mm) lies well outside the spectral range of the photodiode, and is therefore invisible to it. Fig. 7 shows a schematic of the sensing arrangement used. The signals obtainable from the photodiode are dependent on a number of factors (Li, I990),

Condition	Power (W)	Speed (mm/s)
1	600	10
2	600	20
3	600	30
4	800	10
5	800	20
6	800	30
CW CO_2, TEM_{00}, focal spot 250 µm, O_2 2.7 bar, mild steel of 1 mm thick.		

TABLE 1 EXPERIMENTAL CONDITIONS

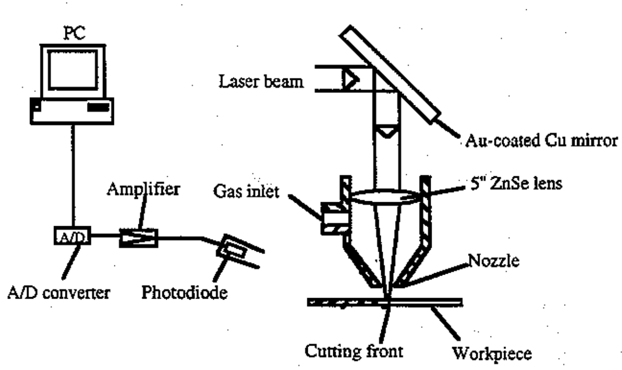

FIG. 7 SCHEMATIC DIAGRAM OF THE SENSING SYSTEM

$$V_p = K_s\, \varepsilon\, A_f \cos(\gamma)\, T^4 / d_s^2 \qquad (3)$$

where K_s is diode sensor constant, A_f effective diode viewing area, γ sensor angle, d_s duct diameter. Assuming the sensor constant, viewing area, sensor angle and distance remain relatively uniform, then the signal output is basically affected by emissivity and temperature. Because temperature represents a fourth-power relationship (coupled with the high temperatures experienced in laser cutting), the photodiode signal will therefore be strongly dominated by cutting front temperature fluctuations. The signals obtained from the photodiode were initially captured on a digital spectrum analyzer to examine all frequency components up to 25 kHz. A cutoff frequency of 2000 Hz was set, although striation frequencies above a few hundred hertz are generally uncommon. Experiments were carried under the conditions listed in Table 1.

SIGNAL PROCESSING AND COMPARISON

Typical photodiode signals are shown in Fig. 8 and their power spectral density (PSD) plots shown in Fig. 9. Although peaks are identifiable, they tend to span over bands. An alternative parametric method, dispersion analysis (DA), is also used (Appendix II). Randomness in the signal is due to many contributing factors such as changes in the melt pool size, shape and emissivity. Dynamics of the signal on the other hand will be due to the cyclic forming of striations. Via the dispersion analysis, dispersion percentages were obtained which describe the relative contribution of the frequencies in the signal. Fig. 10 compares the results obtained from both the spectral and parametric analysis of the photodiode signal with stylus-measured striation frequencies. It is seen that they correlate well. Fig. 10 also shows the dominant dispersion frequencies, the results of which correspond closer to the actual striation frequencies measured than those from the spectral analysis. This methodology has brought about a more sensitive feature extraction technique because power spectrums provide only qualitative information, whilst dispersion analysis gives quantitative information. The modeling process on which the dispersion analysis is based also provides smoothing of the original data. This inherent filtering characteristic has been beneficial in extracting striation frequency from laser cutting light emissions.

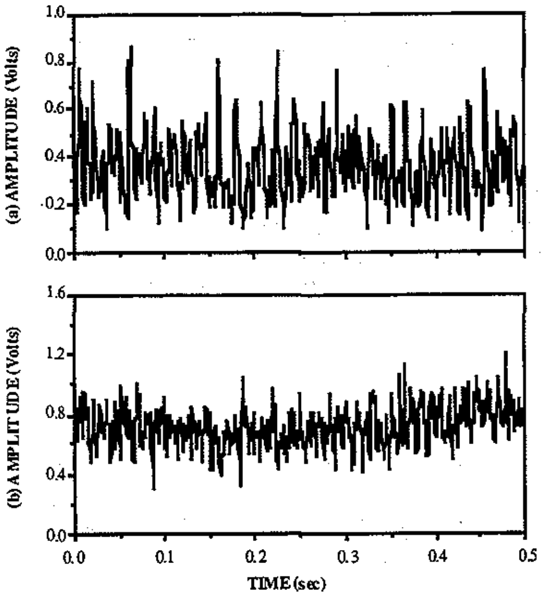

FIG. 8 TYPICAL PHOTODIODE SIGNALS (A) POWER 600 W, SPEED 10 mm/s, (B) 600 W, 20 mm/s

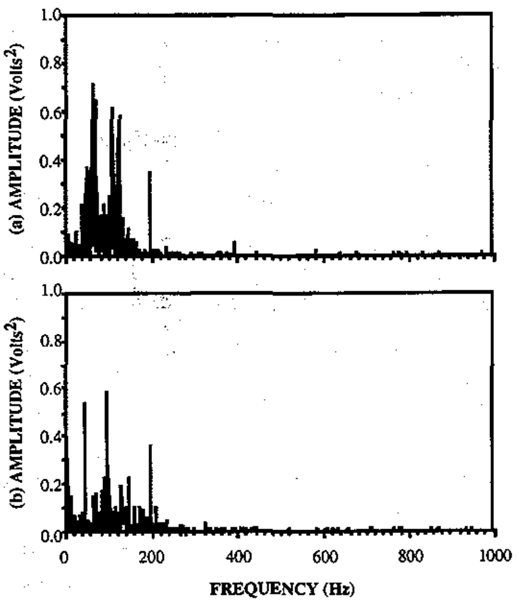

FIG. 9 TYPICAL POWER SPECTRUMS OF THE PHOTODIODE SIGNALS (A) POWER 600 W, SPEED 10 mm/s, (B) 600 W, 20 mm/s

It is also desirable to compare the results with theoretical one. Most work on striation formation to date is qualitative except an effort by Schuocker (1986, 1987). The model is based on dynamic energy and a perturbation treatment led to an expression of striation frequency (Appendix I). Such an analytical result is shown in Fig. 11 (Di Pietro & Yao, 1995). Since frequencies estimated from photodiode signal agree with measured ones (Fig. 10) and measured ones agree with the theoretical one, it is reasonable to conclude the photodiode based frequencies also agree with the theoretical ones.

The peak strengths at striation frequency are related with the measured maximal roughness heights. As seen from Fig. 12, the peak strengths change in the same manner as the maximal roughness heights do, that is, they increase or decrease with the roughness heights. The proportional coefficient, however, appears to be dependent on cutting conditions and the relationship tends to be complex.

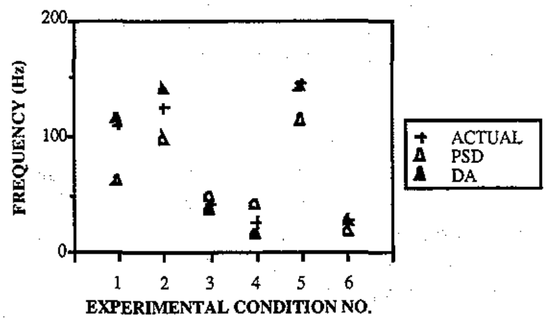

Fig. 10 RESULTS FROM SPECTRAL AND PARAMETRIC DISPERSION ANALYSIS COMPARED TO STRIATION FREQUENCIES MEASURED

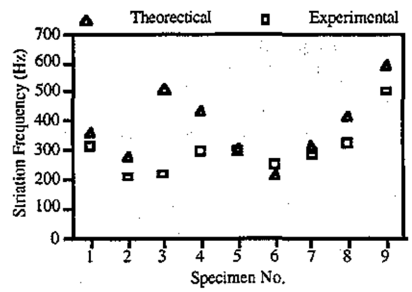

FIG. 11 EXPERIMENTAL RESULTS COMPARED TO THEORETICAL CALCULATION (DI PIETRO & YAO, 1995)

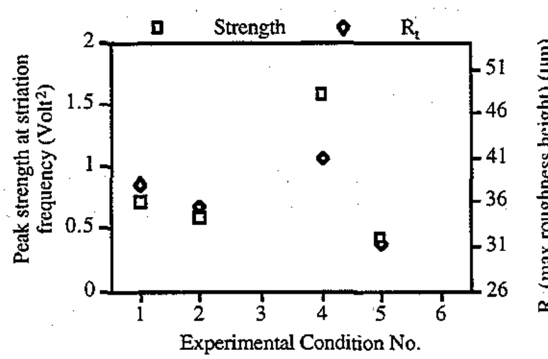

FIG. 12 PEAK STRENGTHS AT STRIATION FREQUENCY AND MEASURED ROUGHNESS HEIGHT

CONCLUDING REMARKS

Surface quality is predicted during the cutting operation. This is important in un-manned operation of such systems and can alert operators of failing quality. Both parametric and spectral analysis of light emission signals from a photodiode sensor are sensitive means to extract the underlying dominant frequency mode, with the former method producing closer correlation. Coupled with estimate of roughness heights, quality monitoring is feasible. Hardware FFT analyzers are currently available which can extract information in almost real-time. As far as parametric synthetic decomposition is concerned, algorithms need to be written so that frequency components can be ascertained quickly and efficiently for practical on- line implementation. This is especially true when contour cutting highly complex, intricate parts.

The system shown in Fig. 7 has the benefit of being unintrusive, but unfortunately is dependent on the processing direction taken. To overcome this, a system similar to (Jorgensen, 1991) whereby light emission is detected through the nozzle, could be adopted in practice. This is necessary because contouring tasks are commonly done on laser cutting systems. Nevertheless for the experimental work intended here, uni-directional cutting tests are adequately performed by this system and the methodologies and signal analysis techniques presented are common to both sensing techniques.

Appendix I

Calculation of striation frequency (Schuocker, 1986, 1987, Di Pietro 1995): Using dynamic energy and mass balance equations perturbed around steady state *0*, the frequency of striation ω is calculated as:

$$\omega^2 = \left(\frac{\partial P_{loss}}{\partial T}\right)_0 \left(\frac{\partial m_{loss}}{\partial s}\right)_0 \frac{1}{c_v d^2 b^2 s_0 \rho} \qquad (4)$$

where P_{loss} is energy loss, m_{loss} mass loss, T temperature, s thickness of molten layer, d the workpiece thickness, b kerf width, ρ density of the molten layer and c_v is the volume specific heat capacity. The partial derivative of the energy loss P_{loss} with respect to temperature is:

$$\frac{\partial P_{loss}}{\partial T} = 2\pi d K e^{\frac{-vb}{4\alpha}} / K_0\left(\frac{vb}{4\alpha}\right) + bdv\rho c_v \qquad (5)$$

where K is heat conductivity, α thermal diffusivity, K_0 zero order Bessel function of second kind. The derivative of mass loss is calculated as:

$$\frac{\partial m_{loss}}{\partial s} = \frac{b\rho}{2}\sqrt{\frac{\eta d v_R}{\rho s b}} \qquad (6)$$

where η dynamic viscosity of the reactive gas, v_R velocity of the reactive gas. The steady state molten layer thickness s_0 is calculated as

$$s_0 = \frac{2\alpha}{v}\left(1 - \frac{T_s}{T}\right)\frac{K_0(vb/4\alpha)}{K_1(vb/4\alpha)} \qquad (7)$$

where K_1 is the first order Bessel function of second kind, T_s melting temperature of workpiece material and T is determined using the result in Fig. 6 on this paper.

Appendix II

The diode signal X_i is processed as a nth-order linear difference system whose eigenvalues are λ_i (i=1, 2, ... n) and whose eigenvectors form a n-by-n orthonormal matrix $\boldsymbol{P}$. The normalized total process fluctuation is decomposed into a summation of dispersions, D_i,

$$1 = E[X_t^2]/\gamma_0 = \sum_{i=1}^{n} D_i = \sum_{i=1}^{n}\sum_{j=1}^{n} g_i \sigma_a g_j / (1 - \lambda_i \lambda_j)\gamma_0 \qquad (8)$$

where γ_0 is process variance, σ_a noise variance, g_i the products of submatrices of $\boldsymbol{P}$ and $\boldsymbol{P}^{-1}$. Value of a D_i represents percentage contribution of the corresponding frequency towards the total process fluctuation. For more details see Di Pietro, 1995.

REFERENCES

Arata, Y., *et al*, (1979), "Dynamic behaviour in laser gas cutting of mild steel", *Trans. JWRI*, Vol. 8(2), pp.15-26.

Biermann, S., et. al., (1988), "Analytical Studies on Laser Cut Surfaces", Proc. of SPIE '88, Vol. 1031, Vienna, Austria, pp. 586-591.

Chen, K., and Yao, Y.L, (1996), "Instabilities in laser cutting process," *Proc. 1997 NSF Design and Manufact. Grantees Conference*, January 7-10, Seattle, WA.

Di Pietro, P., (1995), Characterising, Predicting and optimisating laser cutting quality, *Ph.D. dissertation*, The University of New South Wales, Sydney, NSW, Australia.

Di Pietro, P., and Yao, Y.L., (1994), "An investigation into characterizing and optimizing laser cutting quality - a review", *Int. J. Mach. Tools Manufact.* 34 (2), 225-243.

Di Pietro, P., and Yao, Y.L., (1995), "A new technique to characterize and predict laser cut striations", *Int. J. Mach. Tools Manufact.*, Vol. 35, pp. 993-1001.

Ivarson, A. *et. al.,* (1994), "The oxidation dynamics of laser cutting of mild steel and the generation of striations on the cut edge," *J. of Materials Processing Technology*, Vol. 40, pp. 359-274.

Jorgensen, H., and Olsen, F.O., (1991), "Process Monitoring During CO_2 Laser Cutting, Proc. of SPIE '91, Vol. 1412, Los Angeles, CA, pp. 198-208.

Li, L., *et al.*, (1990), "In-Process Clad Quality Monitoring Using Optical Method", Proc. of SPIE '90, Vol. 1279, Hague, Neth., pp. 89-100.

Schuocker, D., (1986), "Dynamic phenomena in laser cutting and cut quality," *Appl. Phys., B* 40, pp. 9-14, 1986.

Schuocker, D., and Muller, P., (1987), "Dynamic Effects in Laser Cutting and Formation of Periodic Striations", Proc. of SPIE '87, Vol. 801, Hague, Netherlands, pp. 258-264.